Hexagon Shape SIW Bandpass Filter with CSRRs Using Artificial Neural Networks Optimization

Ranjit Kumar Rayala* and Raghavan Singaravelu

Abstract—A dual-band hexagon shape substrate integrated waveguide (SIW) based band-pass filter with single loop complementary spilt ring resonators (CSRRs) is introduced in this paper. The design parameters of this filter are optimized by using artificial neural networks (ANNs). Especially an error back propagation multilayer perceptron (EBP-MLP) neural network with Levenberg-Marquart (LM) algorithm is used. A physical prototype of the proposed model is fabricated and tested. In the lower passband from 10.2 to 10.6 GHz, the insertion loss is about -0.8 dB with a fractional bandwidth of 3.85%, and in the upper passband from 12.11 to 13.31 GHz, the insertion loss is about -0.8 dB with a fractional bandwidth of 9.56%. It is observed that the insertion loss is the same in both the passbands. The obtained experimental results are in good agreement with the estimated results using full-wave analysis and ANN optimization.

1. INTRODUCTION

SIW technology has received a lot of attention because of its advantages like compact size, simple fabrication process, high efficiency, and can be easily integrated with other microwave components and circuits [1]. Miniaturization is a crucial necessity in modern communication systems, hence a SIW bandpass filter was designed and studied using the slow wave approach [2]. SIW structures are often made up of two rows of conducting cylinders or vias implanted in a dielectric substrate that links two parallel metal plates, allowing rectangular waveguide components, printed circuits, active devices, and antennas to be used in planar form [3]. This SIW technology is also widely used for the design and development of spatial filtering applications [4, 5].

The resonators having low insertion loss and high Q-factor are essential elements in modern microwave telecommunication systems particularly in low phase noise oscillators. Three novel dual-band CSRRs have been proposed in order to have low insertion loss and high Q-factor [6]. A dual-band bandpass filter that consists of a SIW dual-mode cavity loaded with two CSRRs on the upper layer has been proposed [7]. The CSRRs have been designed and developed on SIW in order to get band-pass filter characteristics with adjustable bandwidth [8]. A dual-band SIW bandpass filter with single loop CSRRs arrays on the upper layer has been proposed to achieve control over the bandwidth by changing the dimensions of CSRRs and the spacing between CSRRs arrays [9]. Semicircular CSRRs loaded onto the SIW cavity to provide independent control over the passband resonant frequency by varying the ring dimensions have been proposed and investigated [10]. A half-mode substrate integrated waveguide (HSIW) cavity that comprises modified split ring resonators (MSRRs) etched on the top layer of the waveguide has been proposed and investigated [11]. A SIW dual-band bandpass filter with a single triangular cavity loaded by complementary triangular spilt ring resonators (CTSRRs) and having three transmission zeros (TZ) in the overall passband has been proposed [12]. A pair of S-shaped

---

complementary spiral resonators (S-CSRs) on the upper layer of the HMSIW cavity have been used to improve selectivity and generate transmission zeros near the passband [13]. The resonant frequencies can be shifted by changing the position and size of the CSRR in a sixteenth-mode substrate integrated circular cavity (SM-SICC) band-pass filter that has been proposed [14].

ANN has recently become a major tool in the field of microwave modelling and design [15, 16], and it has been used to reduce simulation time for SIW components, RF circuits, microwave devices, and circuits, all of which require more simulation time to optimize design parameters [17]. The design parameters of X band SIW H-plane bandpass filter have been optimized by using back propagation neural network (BPNN) proposed [18]. To optimize the SIW filter parameters, a novel neural network of calibrated coarse model has been proposed, and some training data have been used to synthesize the entire SIW filter [19]. To provide a quick and precise frequency response, the scattering parameter S_{21} in dB has been predicted using a multi-layer perceptron MLP-ANN [20]. A semi-supervised radial basis function neural network (SS-RBFNN) model has been proposed that uses an enhanced sampling strategy to reduce the uneven error distribution and slow convergence caused by sample selection uncertainty in the training process of artificial neural networks [21].

In this paper, a hexagon shape bandpass filter is proposed, and the filter parameters are optimized using MLP-ANN. Levenberg-Marquart (LM) algorithm is used to train the neural network. The keyword used is 'trainlm' in the MATLAB. The learning rate is 0.01, and the used activation function is log-sigmoid. The ANN results and CST Microwave studio simulated results are in good agreement.

This paper consists of five sections. The basic topology design methodology of proposed filter is explained in Section 2. The optimization of filter parameters using neural networks is explained in Section 3. The simulation results are explained in Section 4. The fabrication process and measurement setup are explained in Section 5.

2. DESIGN OF SIW BPF

The CST microwave studio is used to develop and simulate the hexagon-shaped bandpass filter depicted in Figure 1. The basic structure consists of three layers, and the bottom and top layers are perfect electric conductors (PECs). The middle layer of the SIW structure is made of Roggers RO4003C, which has a dielectric constant (ε_r) of 3.55 and substrate height (h) of 0.81 mm. The hexagon shape is modelled on the top PEC with a diameter (H_{dia}). Two square-shaped slots are etched on the opposite sides of the hexagon along the longitudinal direction. While microstrip feeding is given on both sides, these two square slots are used as feed points.

In order to make it as a SIW topology, the vias are arranged along the hexagon shape with a separation distance (p) and a diameter (d). From upper PEC these vias are penetrated through the dielectric material and the lower PEC. Two single layer Complimentary Split Ring Resonators (CSRR)
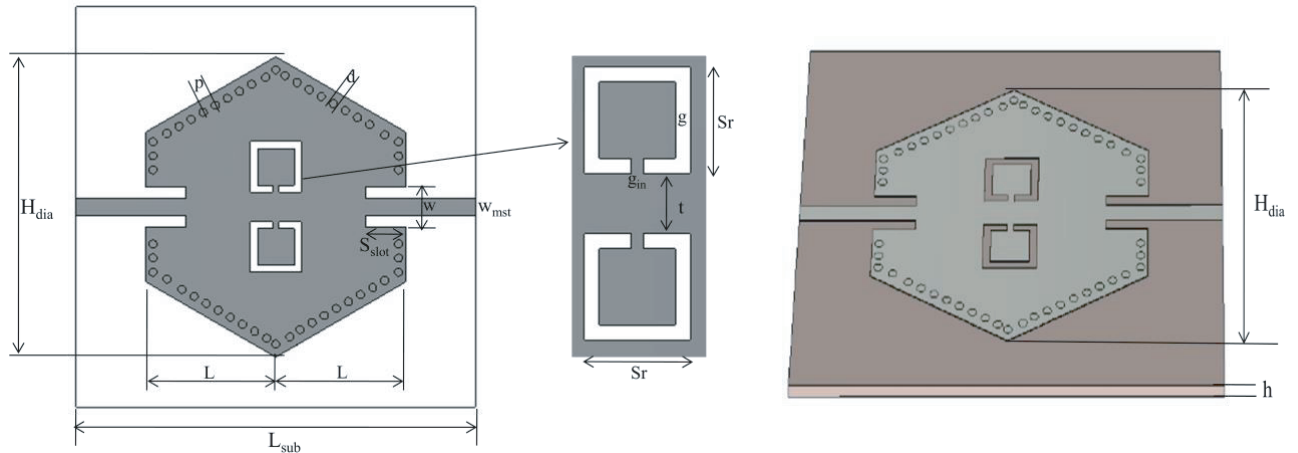

Figure 1. Topology of proposed filter.

are etched on the upper PEC. The optimised values for this hexagon shape topology are shown in Table 1.

Table 1. Dimensions of the proposed filter.

S. No.	Parameter	Value (mm)
1	d	0.8
2	H_{dia}	30
3	g	1
4	g_{in}	0.6
5	h	0.81
6	L	26
7	L_{sub}	40
8	p	1.4
9	S_{slot}	4
10	S_r	3.6
11	t	0.8
12	w	4
13	W_{mst}	1.74

3. BASIC MODEL OF BP-ANN

Neural networks play an important role in many engineering problems, so these networks are used in the filter parameters optimization. There are many types of neural networks available like multilayer feed forward neural networks (MLP-ANN), Temporal NN, radial basis function networks (RBF), Wavelet NN, and Self organizing maps [20]. Error back propagation multilayer perceptron artificial neural network (BP-MLP-ANN) is the most widely used network.

A neural network (NN) contains three layers, namely input layer, hidden layer, and output layer. The physical parameters that are intended to optimize are treated as input layer neurons. The second layer consists of a number of sub-layers which is known as the hidden layer, and finally, the output layer contains one or more neurons. Neurons are nothing but the information processing units, and they are also known as nodes or base points. The basic model of neural network is as shown in Figure 2.
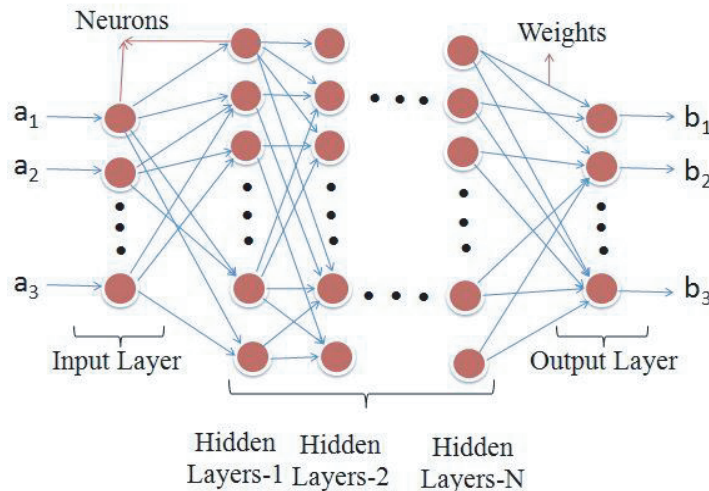

Figure 2. Basic model of Neural Network.

The links between neurons from input layer to output layer through the hidden layer are known as interconnections or weights.

In order to optimize the filter parameters, a supervised learning mechanism is used. In this method, the neural network must be trained with a set of known values, which are known as training data shown in Table 2, and this process is known as training of neural network. In the training process, the weights of the network are adjusted themselves to produce an output with a minimum mean square error (MSE). Now another set of data known as testing data shown in Table 3 is used to test the trained network. These two data sets are generated from the CST Microwave Studio by performing a number of simulations.

Table 2. Training data.

S. No.	S_{Slot} (mm)	S_{11} (dB) (CST)
1	3.95	-20.291
2	4.03	-19.616
3	4.05	-19.235
4	4.15	-17.367
5	4.18	-16.848
6	4.25	-15.921
7	4.35	-13.335
8	4.45	-12.448
9	4.55	-12.075
10	4.65	-11.233

Table 3. Testing data.

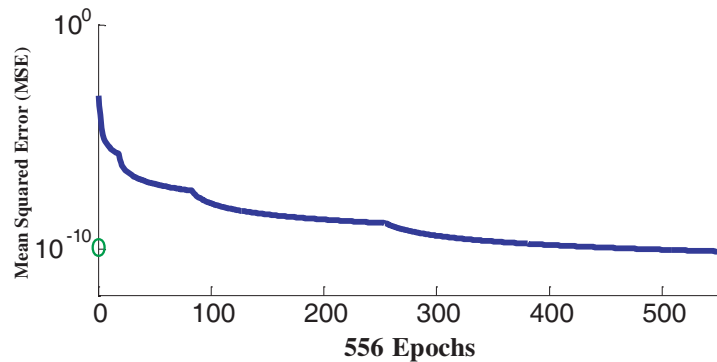| S. No.	S_{Slot} (mm)	S_{11} (dB) (CST)	S_{11} (dB) (ANN)	Mean Square Error
1	3.98	-20.415	-20.1313	0.2837
2	4.0	-20.673	-20.3526	0.3204
3	4.1	-18.276	-18.1666	0.1094
4	4.2	-16.670	-16.9877	0.3177
5	4.3	-15.004	-14.9313	0.0727
6	4.33	-13.598	-13.5915	0.0065
7	4.4	-12.863	-12.4525	0.4105
8	4.5	-12.078	-11.9968	0.0812
9	4.6	-11.622	-11.2806	0.3414

Figure 3. Training performance of the neural network.

The proposed neural network in this paper is a single hidden layer feed forward neural network, which comprises an input layer, a hidden layer, and an output layer, each having a number of neurons of 1, 10, and 1, respectively. The hidden layer neurons are fixed by trial and error method. Levenberg-Marquart (LM) algorithm is used to train the neural network. The keyword used is 'trainlm' in the MATLAB. The learning rate is 0.01, and the activation function used is log-sigmoid. Figure 3 shows the MSE plotted against the number of epchos, and the training performance of proposed neural network can be observed from this plot.

4. SIMULATION RESULTS DISCUSSION

The proposed hexagon shape dual bandpass filter, depicted in Figure 1, was designed and simulated using CST MWS, with simulated results presented in Figure 4. This graph shows the variation of S_{11} and S_{12} w.r.t frequency. The designed filter shows dual-band characteristics. The lower passband shows a narrow band response with a centre frequency of 10.41 GHz and offers a bandwidth of 403 MHz (ranging from 10.2 to 10.6 GHz). The proposed filter has another passband which is a wide-band response centred at 12.55 GHz. The upper passband provides a good wide-band response with a transmission bandwidth of 1.2 GHz (from 12.11 to 13.31 GHz). The return loss in lower passband is about -23 dB with a
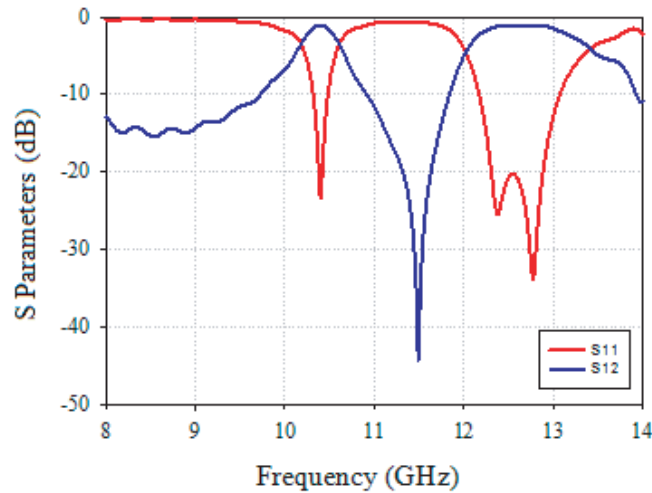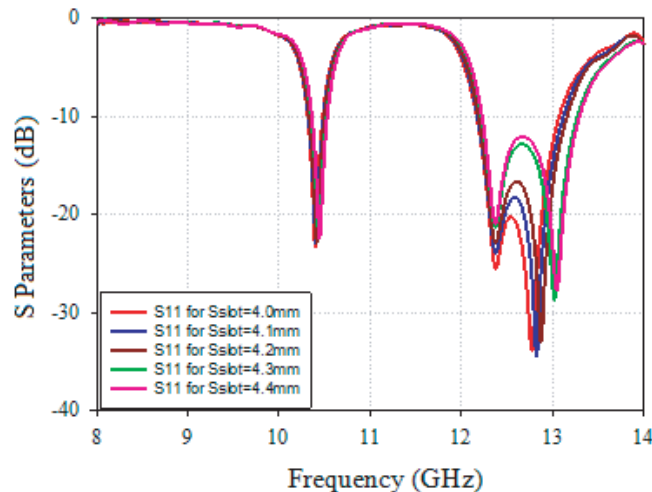

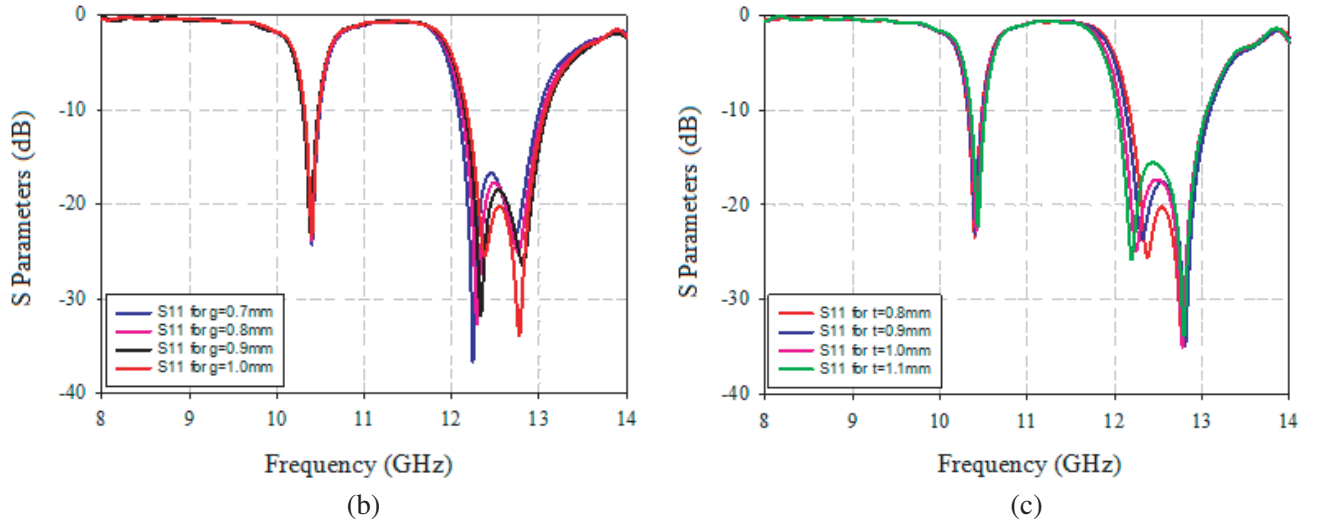**Figure 4.** Frequency response of proposed filter.

(a)

(b)

(c)

Figure 5. (a) Parametric analysis with respect to S_{slot}. (b) Parametric analysis with respect to 'g'. (c) Parametric analysis with respect to 't'.

fractional bandwidth of 3.84%, and in higher pass band it is about $-20.4\,$dB with a fractional band width of 9.56%. Figures 5(a)–5(c) present the parametric analysis of the proposed filter. By varying different parameters like S_{slot}, g and t, the parametric analysis was carried out in order to generate training data for ANN.

Throughout the overall frequency band of operation, it offers an insertion loss of $0.8\,$dB. From the frequency response we can observe three transmission poles. One is at the first resonant frequency (fr_1) of $10.4\,$GHz in the lower passband, and the other transmission poles are in the upper passband at the second resonant frequency (fr_2) of $12.38\,$GHz and the third resonant frequency (fr_3) of $12.77\,$GHz. The electric field distribution of designed bandpass filter is shown in Figure 6 which is obtained in CST MWS while the simulation is carried out. The colour ramp represents the variation in electric field strength, and the proposed filter shows the dominant mode behaviour as normal rectangular waveguide.
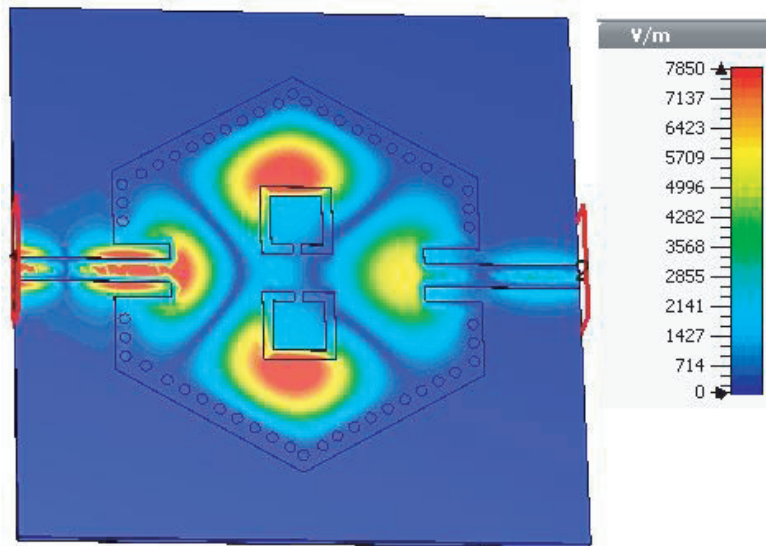

Figure 6. Electric field distribution.

5. FABRICATION AND EXPERIMENTAL VALIDATION

Figure 7 shows the fabricated model of the proposed filter, and Figure 8 shows the total measurement setup. Simple printed circuit board (PCB) process is used to design the proposed bandpass filter which shows two passbands. The dielectric substrate used is Rogers RO4003C of height 0.81 mm, having a relative permittivity (ε_r) of 3.55 and magnetic loss tangent $\tan(\delta)$ of 0.0027. During the fabrication process of the proposed filter, at first the copper coating was done on both sides of the dielectric material. After that to make it into a SIW structure, via holes have been drilled. These via holes are placed in hexagon shape as shown in Figure 7. Finally from the upper PEC layer, a portion of PEC was removed in order to form CSRR slots. The Combinational Analyzer (Anritsu-MS2037C) has been used to measure this prototype model.
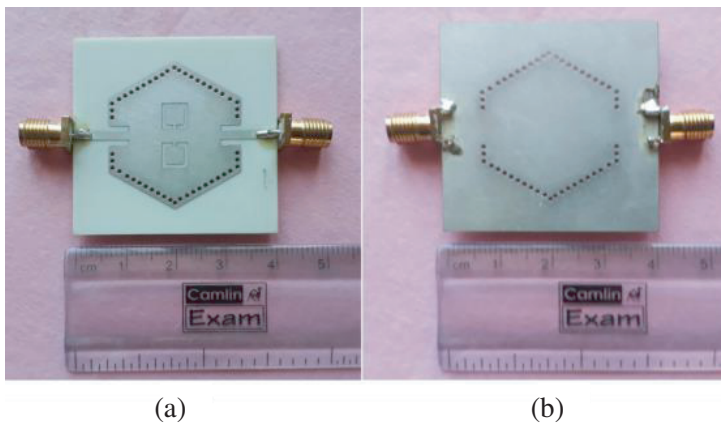

Figure 7. Photographs of fabricated models. (a) Top view. (b) Bottom view.

Figure 8. Measurement setup.

The measured results were plotted against the simulated ones, and they are in good agreement as shown in Figure 9. At -10 dB, in the lower passband and upper passband the measured S_{11} is shifted by 126 MHz and 90 MHz respectively from the simulated results.

From Figure 9, the simulated and measured transmission coefficients S_{12} show an insertion loss of
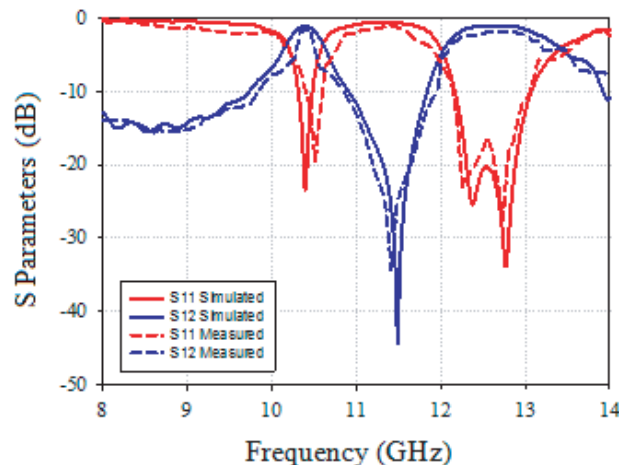

Figure 9. Simulated results plotted against measured results.

-0.8 dB and -1.55 dB, respectively, in the lower passband and upper passband which are about -0.8 dB and -1.62 dB, respectively. This difference in insertion loss is because losses due to SMA connectors were not considered while the simulation is performed.

6. CONCLUSION

A dual-band hexagon shape SIW bandpass filter with single loop CSRR based on ANN is presented. The design parameters of this filter are optimized by using an EBP-MLP neural network with LM algorithm and investigated using full-wave analysis with CST microwave studio. To prove the efficacy of the proposed model, a prototype is fabricated, and its functionality is verified experimentally. The measured insertion loss in the lower passband is about -1.55 dB and in the upper passband it is about -1.62 dB. The measured and simulated results are in good agreement and are also in good agreement with the ANN results with minimum mean square error. The properly trained neural networks give results at a faster rate than any other commercial CAD tools. The results are encouraging and useful for the easy optimization of SIW circuits with reduced computational complexity and execution time.

ACKNOWLEDGMENT

REFERENCES

1. Deslandes, D. and K. Wu, "Single-substrate integration technique of planar circuits and Waveguide filters," *IEEE Transactions on Microwave Theory and Techniques*, Vol. 51, No. 2, 593–596, 2003.

2. Ananya, P., P. Athira, and S. Raghavan, "Miniaturized band pass filter in substrate integrated waveguide technology," *International Journal of Engineering & Technology*, Vol. 7, No. 3.13, 95–98, 2018.

3. Krushna Kanth, V. and S. Raghavan, "EM design and analysis of a substrate integrated waveguide based on a frequency-selective surface for millimeter wave radar application," *J. Comput. Electron.*, Vol. 18, 189–196, 2019.

4. Krushna Kanth, V. and S. Raghavan, "Ultra thin wide band slot and patch FSS elements with sharp band edge characteristics," *International Journal of Electronics*, Vol. 107, 1365–1385, 2020.

5. Krushna Kanth, V. and S. Raghavan, "A novel Faraday-cage inspired FSS shield for stable resonance performance characteristics," *International Journal of Electronics Letters*, Vol. 8, 60–69, 2020.

6. Hamidkhani, M., R. Sadeghi, and M. Karimi, "Dual-band high Q-factor complementary split-ring resonators using substrate integrated waveguide method and their applications," *Journal of Electrical and Computer Engineering*, Vol. 2019, 11, 2019.

7. Hao, Z., K. Wei, and W. Wen, "Dual-band substrate integrated waveguide bandpass filter utilizing complementary split ring resonators," *Electronics Letters*, Vol. 54, 85–87, 2018.

8. Park, W.-Y. and S. Lim, "Bandwidth tunable and compact BandPass Filter (BPF) using Complementary Split Ring Resonators (CSRRS) on Substrate Integrated Waveguide (SIW)," *Journal of Electromagnetic Waves and Applications*, Vol. 24, No. 17–18, 2407–2417, 2010.

9. Li, D., J.-A. Wang, Y. Yu, Y. Liu, Z. Chen, and L. Yang, "Substrate integratedwaveguide-based complementary split-ring resonator and its arrays for compact dual-wideband bandpass filter design," *Int. J. RF Microw. Comput. Aided Eng.*, Vol. 31, e22504, 2021.

10. Chaudhury, S. S., S. Awasthi, and R. K. Singh, "Dual passband filter based on semi circular cavity substrate integrated waveguide using complementary split ring resonators," *IEEE Applied Electromagnetics Conference (AEMC)*, 1–2, Aurangabad, India, 2017.

11. Yan, T. and X.-H. Tang, "Substrate integrated waveguide dual-band bandpass filter with complementary modified split-ring resonators," *IEEE International Wireless Symposium (IWS 2015)*, 1–4, Shenzhen, China, 2015.

12. Geng, Q. F., H. J. Guo, Y. Y. Zhu, W. Huang, S. S. Deng, and T. Yang, "A novel dual-band filter based on single-cavity CTSRR loaded triangular substrate-integrated waveguide," *International Journal of Microwave and Wireless Technologies*, Vol. 11, 894–898, 2019.

13. Wei, F., H. J. Yue, J.-P. Song, H. Y. Kang, and B. Li, "Half-mode SIW BPF loaded with S-shaped complementary spiral resonators," *Progress In Electromagnetics Research Letters*, Vol. 77, 13–18, 2018.

14. Chen, X.-G., G. H. Li, Z. Shi, and S. D. Feng, "Compact SICC dual-band and UWB filters using multimode technology," *Progress In Electromagnetics Research Letters*, Vol. 92, 69–74, 2020.

15. Zhang, Q.-J., K. C. Gupta, and V. K. Devabhaktuni, "Artificial neural networks for RF and microwave design — from theory to practice," *IEEE Transactions on Microwave Theory and Techniques*, Vol. 51, No. 4, 1339–1350, 2003.

16. Rayas-Sanchez, J. E., "EM-based optimization of microwave circuits using artificial neural networks: The state-of-the-art," *IEEE Transactions on Microwave Theory and Techniques*, Vol. 52, No. 1, 420–435, Jan. 2004.

17. Angiulli, G., E. Arnieri, D. De Carlo, and G. Amendola, "Feed forward neural network characterization of circular SIW resonators," *IEEE Antennas and Propagation Society International Symposium*, 1–4, San Diego, CA, USA, 2008.

18. Tabatabaeian, Z. S. and M. H. Neshat, "Design investigation of an X-band SIW *H*-plane band pass filter with improved stop band using neural network optimization," *Applied Computational Electromagnetics Society Journal*, Vol. 30, No. 10, 1083–1088, 2015.

19. Du, G.-Y. and L. Jin, "Neural network of calibrated coarse model and application to substrate integrated waveguide filter design," *International Journal of RF and Microwave Computer-Aided Engineering*, Vol. 30, No. 10, e22374, 2020.

20. Amir, B. and B. S. Masoud, "Optimal design of double folded stub microstrip filter by neural network modelling and particle swarm optimization," *Journal of Microwaves, Optoelectronics and Electromagnetic Applications*, Vol. 11, 204–213, 2012.

21. Xiao, L., W. Shao, F. Jin, B. Wang, W. T. Joines, and Q. H. Liu, "Semi supervised radial basis function neural network with an effective sampling strategy," *IEEE Transactions on Microwave Theory and Techniques*, Vol. 68, 1260–1269, 2020.